# Poly(ADP-ribose) polymerase 1 (PARP1) promotes oxidative stress–induced association of Cockayne syndrome group B protein with chromatin

Received for publication, June 22, 2018, and in revised form, September 25, 2018 Published, Papers in Press, September 28, 2018, DOI 10.1074/jbc.RA118.004548

**Erica L. Boetefuer**[‡§1], **Robert J. Lake**[‡1,2], **Kostiantyn Dreval**[‡2], **and Hua-Ying Fan**[‡2,3]

*From the* [‡]*Department of Internal Medicine, Division of Molecular Medicine, Program in Cancer Genetics, Epigenetics, and Genomics, University of New Mexico Comprehensive Cancer Center, Albuquerque, New Mexico 87131 and the* [§]*Department of Biology, University of Pennsylvania, Philadelphia, Pennsylvania 19104*

Edited by Joel M. Gottesfeld

**Cockayne syndrome protein B (CSB) is an ATP-dependent chromatin remodeler that relieves oxidative stress by regulating DNA repair and transcription. CSB is proposed to participate in base-excision repair (BER), the primary pathway for repairing oxidative DNA damage, but exactly how CSB participates in this process is unknown. It is also unclear whether CSB contributes to other repair pathways during oxidative stress. Here, using a patient-derived CS1AN-sv cell line, we examined how CSB is targeted to chromatin in response to menadione-induced oxidative stress, both globally and locus-specifically. We found that menadione-induced, global CSB–chromatin association does not require CSB's ATPase activity and is, therefore, mechanistically distinct from UV-induced CSB–chromatin association. Importantly, poly(ADP-ribose) polymerase 1 (PARP1) enhanced the kinetics of global menadione-induced CSB–chromatin association. We found that the major BER enzymes, 8-oxoguanine DNA glycosylase (OGG1) and apurinic/apyrimidinic endodeoxyribonuclease 1 (APE1), do not influence this association. Additionally, the level of γ-H2A histone family member X (γ-H2AX), a marker for dsDNA breaks, was not increased in menadione-treated cells. Therefore, our results support a model whereby PARP1 localizes to ssDNA breaks and recruits CSB to participate in DNA repair. Furthermore, this global CSB–chromatin association occurred independently of RNA polymerase II–mediated transcription elongation. However, unlike global CSB–chromatin association, both PARP1 knockdown and inhibition of transcription elongation interfered with menadione-induced CSB recruitment to specific genomic regions. This observation supports the hypothesis that CSB is also targeted to specific genomic loci to participate in transcriptional regulation in response to oxidative stress.**

Cockayne syndrome is a devastating recessive disorder characterized by features of premature aging, extreme sun sensitivity, and neurological and developmental abnormalities (1, 2). The majority of Cockayne syndrome cases are the result of mutations within the gene encoding Cockayne syndrome protein B (CSB),[4] an ATP-dependent chromatin remodeler (3–5). CSB plays a role in transcription regulation (6–11) and is essential for transcription-coupled nucleotide excision repair (TC-NER) (3, 12–17). CSB also contributes to the relief of oxidative stress by regulating DNA repair as well transcription (18–20); however, the mechanisms underlying these activities remain elusive. Cells deficient in CSB show increased sensitivity to oxidizing agents (20–22), accumulate oxidative DNA damage (22, 23), and display increased levels of intracellular reactive oxygen species (ROS) (21).

The major repair pathway for oxidative DNA damage is base-excision repair (BER) (24). BER is initiated by a substrate-specific DNA glycosylase that removes the oxidized base. This is followed by cleavage of the sugar-phosphate backbone and excision of the remaining apurinic-apyrimidinic site by apurinic-apyrimidinic endonuclease 1 (APE1) or, in some cases, glycosylases with inherent endonuclease activity. The resulting nicked DNA is recognized by and activates poly(ADP-ribose) polymerase 1 (PARP1), which uses $NAD^+$ to catalyze the addition of poly(ADP-ribose) (PAR) polymers to itself as well as other proteins. PARP1 is hypothesized to recruit proteins important for DNA repair, such as the scaffold protein XRCC1. PARP1 may also serve to stabilize nicked DNA, preventing degradation of single-strand breaks into double-strand breaks (24–28). The remaining gap is filled by DNA polymerase β, and ligation is performed by DNA ligase IIIα (Lig3). An alternative pathway, long-patch BER, is initiated by blocked 5′-ends during nick repair.

This work was supported by National Institutes of Health Grants GM115888 (to H. Y. F.) and T32 GM-07229 (to E. L. B.). The authors declare that they have no conflicts of interest with the contents of this article. The content is solely the responsibility of the authors and does not necessarily represent the official views of the National Institutes of Health.

This article contains Figs. S1–S6 and Table S1.

[1] Both authors contributed equally to this work.

[2] These authors were supported in part by Cancer Center Support Grant P30CA118100.

[3] To whom correspondence should be addressed: Dept. of Internal Medicine, University of New Mexico-Health Science Center, Albuquerque, NM 87131. Tel.: 505-272-1085; E-mail: hufan@salud.unm.edu.

[4] The abbreviations used are: CSB, Cockayne syndrome protein B; TC-NER, transcription-coupled nucleotide excision repair; BER, base-excision repair; APE1, apurinic-apyrimidinic endonuclease 1; PARP1, poly(ADP-ribose) polymerase 1; PAR, poly(ADP-ribose); OGG1, oxoguanine glycosylase 1; CTCF, CCCTC–binding transcription factor; RNA pol II, RNA polymerase II; DRB, 5,6-dichloro-1-β-D-ribofuranosylbenzimidazole; DMSO, dimethyl sulfoxide; BRG1, brahma-related gene-1; XRCC1, X-ray repair cross-complementing protein 1; shRNA, short hairpin RNA; GAPDH, glyceraldehyde-3-phosphate dehydrogenase; qPCR, quantitative real-time PCR; FBS, fetal bovine serum; DMEM, Dulbecco's modified Eagle's medium; BisTris, 2-[bis(2-hydroxyethyl)amino]-2-(hydroxymethyl)propane-1,3-diol; HRP, horseradish peroxidase.

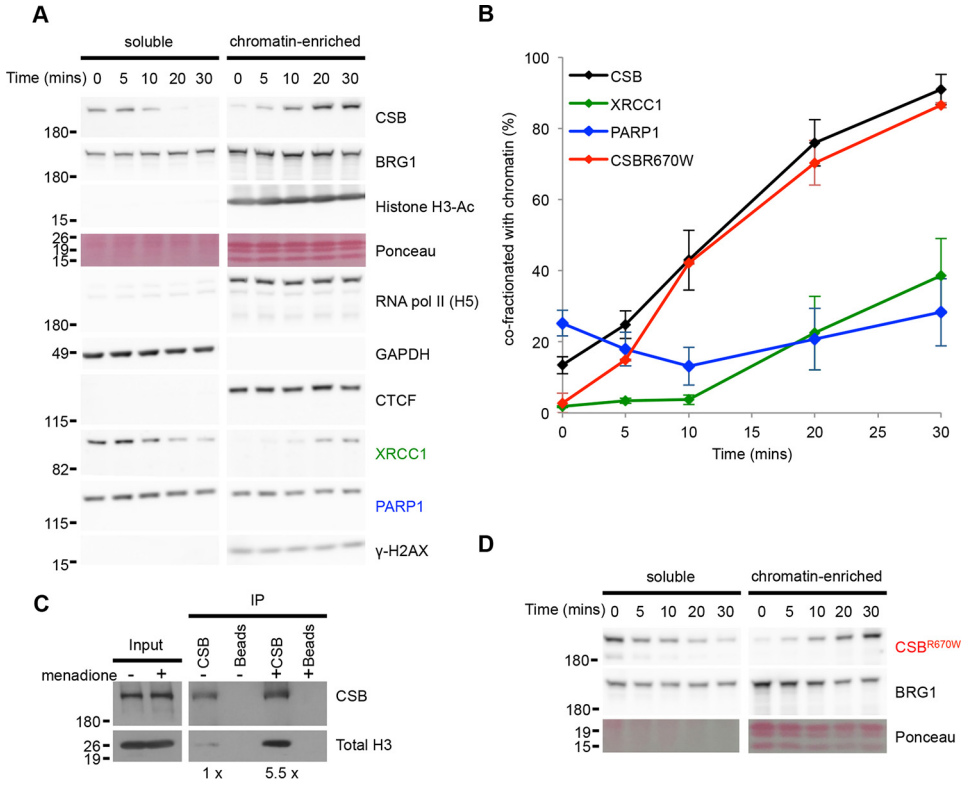


**Figure 1. The association of CSB with chromatin in response to menadione treatment occurs independently of ATP hydrolysis.** *A*, protein fractionation assay in CS1AN-CSB$^{WT}$ cells following treatment with 100 $\mu$M menadione for times indicated. Western blots were probed with antibodies listed. BRG1 was used as a loading control. Acetylated histone H3 and total core histones (visualized by Ponceau S staining) were used as markers for the chromatin-enriched fraction. GAPDH was used as a marker for the soluble fraction. *B*, quantification of percent CSB$^{WT}$ ($n = 5$), PARP1 ($n = 4$), XRCC1 ($n = 4$), and CSB$^{R670W}$ ($n = 2$) in the chromatin-enriched fraction as a function of time, normalized to BRG1. *Error bars* represent S.E. *C*, CSB ChIP-Western blot analysis in CS1AN-CSB$^{WT}$ cells untreated (−) or treated with 100 $\mu$M menadione for 30 min (+). *IP*, immunoprecipitation. *Numbers* at the *bottom* show -fold change in histone H3 normalized to CSB ($n = 2$). *D*, protein fractionation assay in CS1AN-CSB$^{R670W}$ cells following treatment with 100 $\mu$M menadione for times indicated ($n = 2$). Shown is a representative Western blot probed with antibodies to CSB and BRG1 and stained with Ponceau S.

Evidence for the role of CSB in BER has been provided by several groups, which report that cellular extracts from CSB null cells demonstrate reduced incision activity of oxidative DNA lesions *in vitro* (18, 22, 29–31). Recent findings by Menoni *et al.* (32) provide support for the notion that CSB functions in the repair of oxidized DNA by demonstrating that CSB accumulates at sites of locally induced oxidative DNA damage in cells. CSB has also been shown to interact physically and functionally with several key BER proteins such as OGG1 and APE1 (33, 34). Additionally, CSB associates with PARP1, and PARP1 has been shown to poly(ADP-ribosyl)ate CSB (35). Recently, Scheibye-Knudsen *et al.* (36) demonstrated that PARylated PARP1 is required for retaining CSB at sites of oxidative DNA damage and hypothesized that CSB participates in PARP1 displacement from damaged DNA to facilitate repair.

Under replicative cell growth conditions, CSB interacts with chromatin very dynamically, and only ~10% of CSB stably associates with chromatin (37). In response to UV DNA damage, where CSB is employed for TC-NER, the situation is reversed, and ~90% of CSB can become stably associated with chromatin. Recently, we demonstrated that oxidative stress also stabilizes the association of CSB with chromatin on a global level (20). In addition, we found that oxidative stress induces the occupancy of CSB at specific genomic loci, including loci containing the binding motif for the chromatin architectural protein CCCTC–binding transcription factor (CTCF) (20). Importantly, we found that CSB and CTCF reciprocally regulate each other's site-specific chromatin association in response to oxidative stress and that these two proteins interact directly (20). These observations suggest a role for CSB in regulating higher-order chromatin structure during oxidative stress. In the present study, we further characterized the mechanisms by which CSB stably associates with chromatin, both globally and locus-specifically, in response to oxidative stress.

## Results

### *Oxidative stress induces stable CSB–chromatin association*

CSB interacts dynamically with chromatin. During replicative cell growth, ~10% of CSB co-fractionates with chromatin (Fig. 1, *A* and *B*) (20). However, when cells are treated with menadione, which creates oxidative stress by producing reactive oxygen species (38), a substantial increase in CSB–chromatin association is observed (Fig. 1, *A* and *B*) (20). This observation suggests that enhanced CSB–chromatin association results from oxidative stress created by menadione. However, we cannot rule out the possibility that enhanced chromatin association could be associated with another biological consequence of menadione treatment, especially at a relatively high menadione dose (100 $\mu$M). To dissect the mechanisms

by which menadione induces the global association of CSB with chromatin, we used the patient-derived, CSB-deficient CS1AN-sv cell line, stably reconstituted with WT CSB (CS1AN-CSB$^{WT}$) (Fig. S1, *A* and *B*). CSB's expression level in CS1AN-CSB$^{WT}$ cells is within 2-fold of that of the human fibroblast cell line MRC5 (Fig. S1*A*) (39). We examined the time dependence of CSB–chromatin association in CS1AN-CSB$^{WT}$ cells treated with 100 $\mu$M menadione and found that ~90% of CSB co-fractionates with chromatin within 30 min (Fig. 1, *A* and *B*). As demonstrated previously, the partitioning between soluble and chromatin fractions of another ATP-dependent chromatin remodeler, BRG1, was not grossly altered by menadione treatment, and therefore, BRG1 was used as a protein loading control for normalization (Fig. 1*A*) (20). Acetylated histones H3 as well as Ponceau S staining of total histone proteins were used as controls to examine chromatin fractionation efficiency (Fig. 1*A*). Additionally, as expected, the active form of RNA polymerase II was in the chromatin fraction, whereas GAPDH was in the soluble fraction. The CTCF protein, shown previously to increase its association with CSB in response to menadione treatment (20), was chromatin-associated regardless of menadione treatment (Fig. 1*A*).

We next examined how two other DNA repair proteins behaved in this fractionation assay (Fig. 1*A*). Menadione treatment induced the chromatin association of XRCC1, a scaffolding protein involved in DNA repair (Fig. 1, *A* and *B*). We found that PARP1 was present in both the soluble and chromatin fractions, and its partitioning between these two fractions was not significantly changed by menadione treatment (Fig. 1, *A* and *B*). In addition, we did not observe any apparent change in the levels of the classic marker for DNA double-strand breaks, γ-H2AX, after menadione treatment (Fig. 1*A*).

To further demonstrate that oxidative stress increases CSB–chromatin association, we performed anti-CSB chromatin immunoprecipitation (ChIP) followed by Western blot analysis, using an antibody against histone H3. We found a greater than 5-fold increase of histone H3 co-immunoprecipitating with CSB in cells treated with menadione than in untreated cells, demonstrating that menadione treatment increases the association of CSB with chromatin (Fig. 1*C*).

### *ATP hydrolysis by CSB is dispensable for menadione-induced chromatin association*

Stable CSB–chromatin association can also be induced by UV irradiation; this association requires ATP hydrolysis by CSB to relieve autorepression (37). We next determined whether menadione-induced stable CSB–chromatin association is also ATP-dependent. To this end, we used the CSB-deficient CS1AN-sv cell line reconstituted with a CSB protein harboring a patient-derived mutation, CSB$^{R670W}$, which is devoid of ATPase activity (Figs. 1*D* and S1, *A* and *B*) (37). In sharp contrast to UV-induced CSB–chromatin association, menadione-induced stable association of CSB$^{R670W}$ with chromatin was kinetically similar to CSB$^{WT}$. This result reveals that ATP hydrolysis by CSB is dispensable for global CSB–chromatin association in response to menadione treatment.

### *Oxidative stress-induced global CSB–chromatin association is initiated by the N- and C-terminal regions and sustained through the ATPase domain and C-terminal region*

To dissect further the mechanism by which CSB becomes stably associated with chromatin in response to oxidative stress, we analyzed a set of CSB deletion derivatives (Fig. 2). All mutant proteins were stably expressed in CS1AN-sv cells and nuclear (Fig. S1, *A* and *B*) (37). CSBΔN, which is devoid of its N-terminal region but has intact ATPase and C-terminal domains, co-fractionates with chromatin, even in the absence of UV irradiation (37). However, unlike UV-induced CSB–chromatin association, menadione treatment resulted in a further increase in the association of CSBΔN with chromatin (Fig. 2*B*). This result suggests that CSB responds to oxidative stress through its ATPase and/or C-terminal domains.

Deleting the last 484 amino acids of CSB (CSBΔC) abolishes the ability of CSB to associate with chromatin in response to UV irradiation (37). In contrast, CSBΔC still responds to menadione treatment; however, the fraction of CSBΔC associating with chromatin was lower at the 20- and 30-min time points as compared with full-length CSB (Fig. 2*C*), supporting the hypothesis that the C-terminal region contributes to chromatin binding, similar to UV-induced CSB–chromatin association. Increased menadione treatment increased the amounts of CSB-N (CSB$^{1-507}$) that co-fractionated with chromatin, indicating that CSB-N can respond to oxidative stress (Fig. 2*D*). However, CSB-N showed an overall lower chromatin association as compared with CSBΔC (Fig. S1*C*), supporting the notion that the CSB-ATPase domain contributes to stable CSB–chromatin association upon oxidative stress, similar to UV-induced CSB–chromatin association. However, CSB-C alone did not bind chromatin as efficiently as full-length CSB when cells were within the first 10 min of menadione treatment. Nonetheless, CSB-C eventually bound at a level similar to that of full-length CSB, suggesting that CSB-C can also respond to oxidative stress and bind to chromatin, albeit not as efficiently as the full-length protein (Fig. 2*E*). Together these findings support a model in which oxidative stress-induced global CSB–chromatin association is initiated by the N- and C-terminal regions and sustained through the ATPase domain and C-terminal region. Moreover, the results reveal that menadione-induced chromatin association of CSB does not rely upon ATP-dependent relief of autorepression.

### *Menadione-induced, global CSB–chromatin association does not require active transcription by RNA polymerase II*

Another key factor underlying UV-induced CSB–chromatin association is active transcription. The inhibition of RNA polymerase II (RNA pol II) transcription elongation by 5,6-dichloro-1-β-D-ribofuranosylbenzimidazole (DRB) prevents stable CSB–chromatin association induced by UV irradiation (37). We therefore examined whether CSB–chromatin association induced by menadione treatment also requires active RNA pol II transcription. CS1AN-CSB$^{WT}$ cells were exposed to DRB or a DMSO control for 1 h prior to treatment with menadione for 20 min. As demonstrated in Fig. 3, *A* and *B*, DRB did not significantly alter the stable association of CSB with chro-

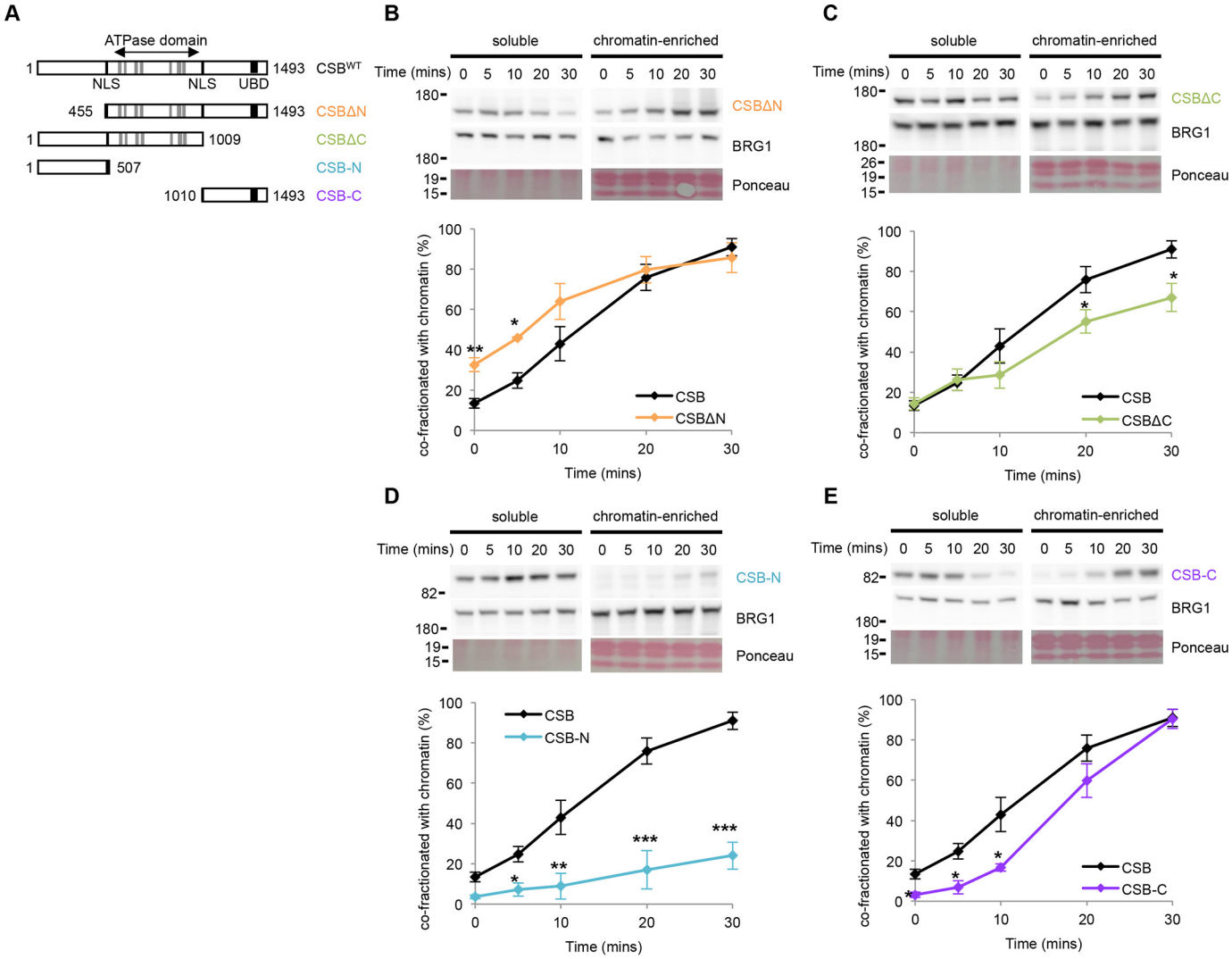


**Figure 2. The association of CSB with chromatin in response to menadione treatment is largely mediated through its ATPase domain and C-terminal region.** *A*, schematic representation of the CSB protein and CSB deletion constructs used in the protein fractionation assays. *Gray boxes* represent the seven conserved helicase motifs, *thin black boxes* represent the two putative nuclear localization signals (*NLS*), and the *thick black box* represents the ubiquitin-binding domain (*UBD*). *B–E*, protein fractionation assays demonstrating chromatin association as a function of time after 100 $\mu$M menadione treatment in CS1AN-sv cells reconstituted with the indicated CSB derivatives: CSB$^{WT}$ ($n = 5$) (from Fig. 1*A*) and CSBΔN ($n = 2$) (*B*), CSBΔC ($n = 3$) (*C*), CSB-N ($n = 2$) (*D*), and CSB-C ($n = 4$) (*E*). Shown are representative Western blots probed with the indicated antibodies and stained with Ponceau S for histones. *Plots* show quantification of the Western blot data with CSB signals normalized to BRG1 signals. *Error bars* represent S.E. Paired *t* tests compare CSB derivative enrichment to CSB$^{WT}$ (*, $p \leq 0.05$; **, $p \leq 0.01$; ***, $p \leq 0.001$).

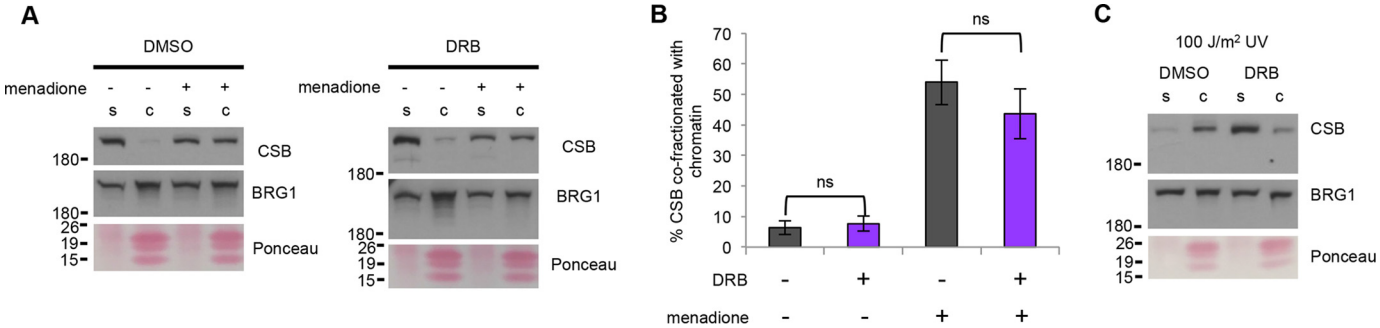


**Figure 3. Inhibiting transcription elongation of RNA pol II by DRB does not alter menadione-induced CSB–chromatin association.** *A*, protein fractionation assay in CS1AN-CSB$^{WT}$ cells. Cells were treated with 50 $\mu$M DRB or DMSO for 1 h followed by a 100 $\mu$M menadione treatment for 20 min. Shown are representative Western blot probed with antibodies listed. *S*, denotes soluble protein fraction; *C*, denotes chromatin-enriched protein fraction. *B*, quantification of CSB chromatin co-fractionation data in *A* normalized to BRG1. Shown are means ± S.E., and paired *t* test compares enrichment in cells with DMSO *versus* DRB treatment ($n = 3$, *ns*, not significant). *C*, protein fractionation assay in CS1AN-CSB$^{WT}$ cells treated with 50 $\mu$M DRB or DMSO for 1 h followed by 100 J/m$^2$ UV irradiation. Cells were analyzed 1 h after UV treatment.

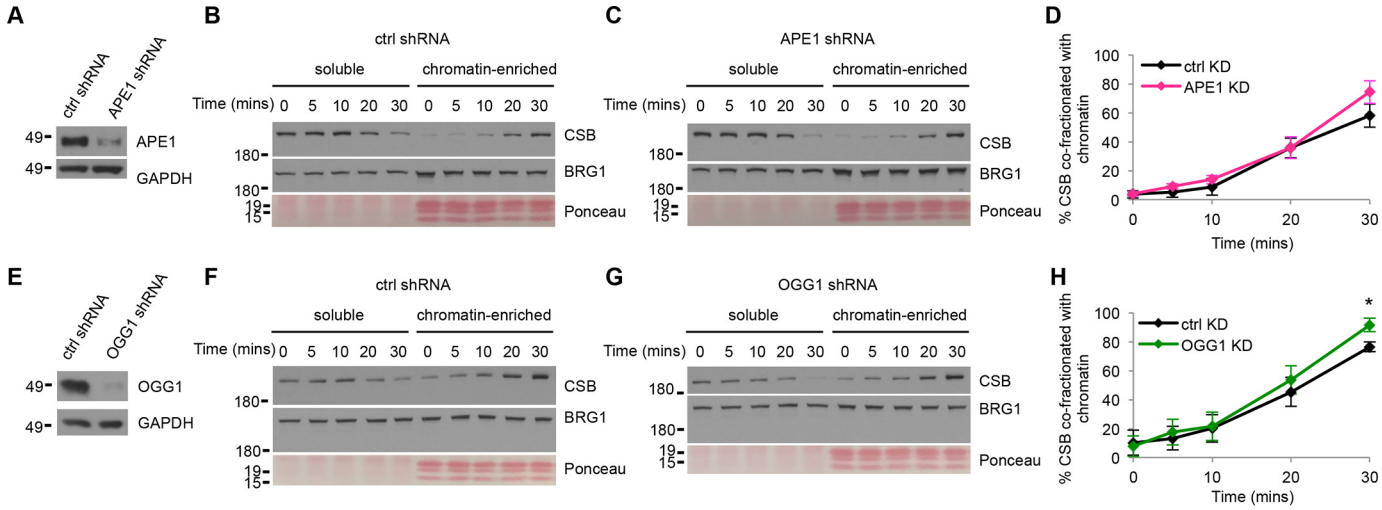


**Figure 4. APE1 or OGG1 are dispensable for menadione-induced global CSB–chromatin association.** *A*, representative Western blots revealing the extent of APE1 knockdown (average knockdown ~72%, normalized to GAPDH). *B* and *C*, protein fractionation assays revealing CSB–chromatin association as a function of time after menadione treatment in CS1AN-CSB$^{WT}$ cells expressing a control (*ctrl*) or APE1 shRNA. Shown are representative Western blots probed with antibodies listed and stained with Ponceau S. *D*, quantification of data in *B* and *C* showing percent CSB co-fractionating with chromatin. *Error bars* represent S.E. Paired *t* test comparing CSB enrichment in control *versus* APE1 knockdown ($n = 4$) revealed no significant differences in association kinetics. *E*, representative Western blots revealing the extent of OGG1 knockdown (average knockdown ~90%, normalized to GAPDH). *F* and *G*, protein fractionation assays revealing CSB–chromatin association as a function of time after menadione treatment in CS1AN-CSB$^{WT}$ cells expressing a control or OGG1 shRNA. Shown are representative Western blots probed with antibodies listed and stained with Ponceau S. *H*, quantification of data in *F* and *G* showing percent CSB co-fractionating with chromatin. *Error bars* represent S.E. Paired *t* test compares CSB enrichment in control to OGG1 knockdown ($n = 4$; *, $p \leq 0.05$).

matin that is induced by menadione on a global level. However, as observed previously, similar DRB treatment prevented UV-induced CSB–chromatin association (Fig. 3*C*). This finding indicates that stable CSB–chromatin association resulting from oxidative stress is regulated by a mechanism that is distinct from UV-induced association.

### *APE1 and OGG1 are dispensable for global menadione-induced CSB–chromatin association*

CSB has been suggested to relieve oxidative stress both by facilitating base-excision repair and regulating the transcription of specific genes. Therefore, menadione-induced global CSB–chromatin association would be expected to represent, to a large degree, sites of oxidized DNA. Accordingly, we used a chromatin fractionation assay to dissect the mechanism by which menadione induces CSB–chromatin association.

As CSB interacts directly with the major apurinic/apyrimidinic endonuclease APE1 (34), we hypothesized that APE1 may recruit CSB to sites of APE1-mediated DNA strand breaks to facilitate APE1 activity in cells treated with menadione. If this hypothesis is correct, we expected to find less CSB co-fractionating with chromatin in cells with decreased APE1 levels. To test this hypothesis, we reduced the level of the APE1 protein using shRNA and determined its consequence on the amount of CSB co-fractionating with chromatin (Fig. 4, *A–D*). As shown in Fig. 4*A*, we were able to reduce APE1 protein levels to less than 30%; however, we did not observe a significant change in menadione-induced CSB–chromatin association. This result suggests that APE1 is unlikely to be essential for global CSB recruitment to chromatin when cells are treated with menadione (Fig. 4, *B–D*).

OGG1, a glycosylase, initiates the base-excision repair of 7,8-dihydro-8-oxoguanine, the major oxidized DNA lesion. Given that CSB has been reported to be in complex with OGG1, we next tested whether the global recruitment of CSB to chromatin is mediated by OGG1. To this end, we reduced OGG1 protein levels using shRNA-targeting OGG1 (Fig. 4*E*) and determined its impact on the levels of CSB co-fractionating with chromatin in response to menadione treatment (Fig. 4, *F–H*). The reduction of OGG1 levels to ~10% did not significantly reduce the level of CSB co-fractionating with chromatin in cells treated with menadione (Fig. 4, *E–H*), arguing against the possibility that OGG1 is essential for the global recruitment of CSB to chromatin when cells are treated with menadione (Fig. 4, *F–H*). However, OGG1 may still function in a more limited capacity of CSB recruitment. Of note, we did observe a small but significant increase in CSB–chromatin association in OGG1 knockdown cells, as compared with control cells, following treatment with menadione for 30 min (Fig. 4*H*). This observation suggests that OGG1 may prevent a fraction of CSB recruitment to chromatin, either directly or indirectly, through a mechanism that awaits to be determined.

Together the findings shown in Fig. 4 argue against the possibility that APE1 or OGG1 play essential roles in the global recruitment of CSB to chromatin upon oxidative stress. Additionally, these results suggest the possibility that CSB may function upstream of these two proteins in base-excision DNA repair.

### *PARP1 facilitates CSB–chromatin association induced by menadione treatment*

Another candidate protein for targeting CSB to chromatin in response to oxidative stress is PARP1, as it interacts with not only CSB but also with poly(ADP)ribosylates CSB (35). Therefore, we examined CSB–chromatin association following control or PARP1 shRNA knockdown (Figs. 5, S2, and S3). Fig. 5*A* is a representative Western blotting showing the level of PARP1 knockdown, which was routinely about 90%. We found that

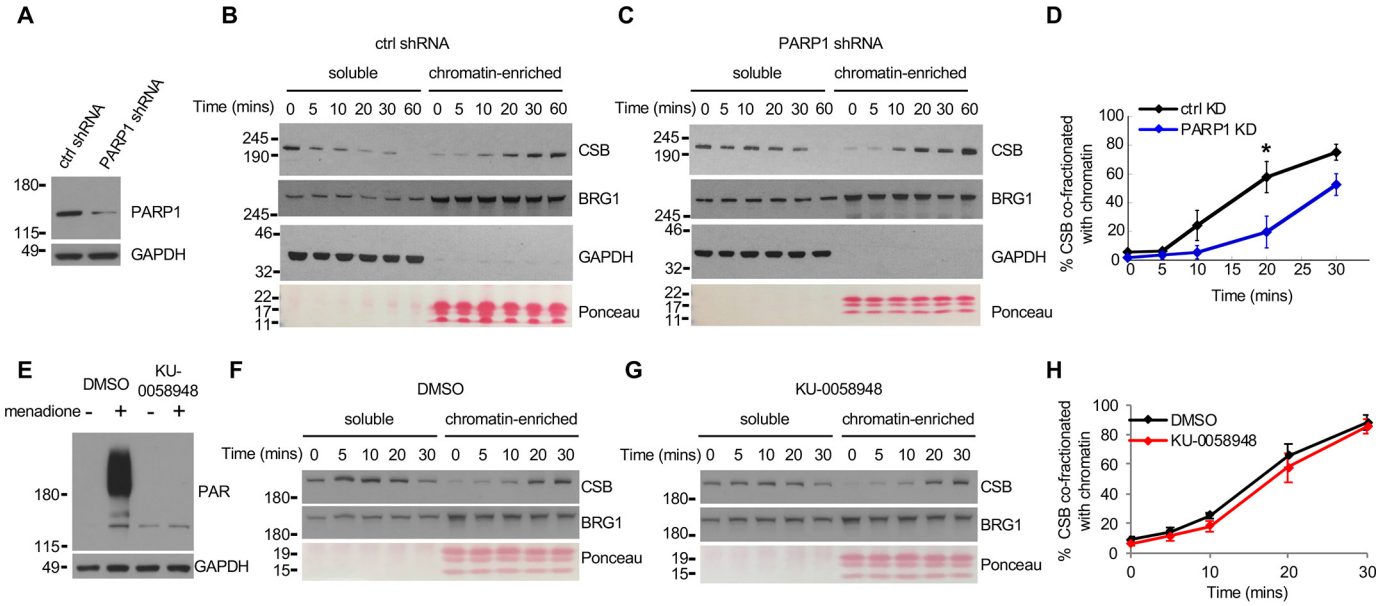


**Figure 5. The PARP1 protein, but not its enzymatic activity, is required for efficient global CSB–chromatin association in response to menadione treatment.** *A*, representative Western blots revealing the extent of PARP1 knockdown (average knockdown ~89%, normalized to GAPDH). *B* and *C*, protein fractionation assays revealing CSB–chromatin association as a function of time after menadione treatment in CS1AN-CSB$^{WT}$ cells expressing a control (*ctrl*) or PARP1 shRNA. Shown are representative Western blots probed with antibodies listed and stained with Ponceau S (the loading ratio of soluble to chromatin is 1:2.2). *D*, quantification of data in *B* and *C* showing percent CSB co-fractionating with chromatin. *Error bars* represent S.E. Paired *t* test compares CSB enrichment in control *versus* PARP1 knockdown ($n = 4$; *, $p \leq 0.05$). *E*, Western blots probed with an anti-PAR antibody demonstrating PARP1 inhibition by KU-0058948. *F* and *G*, protein fractionation assays of CS1AN-CSB$^{WT}$ cells treated with DMSO (vehicle control) or KU-0058948 followed by the addition 100 $\mu$M menadione for the indicated times. Shown are representative Western blots probed with antibodies listed and stained with Ponceau S (the loading ratio of soluble to chromatin is 1:1.25). *H*, quantification of data in *F* and *G* showing percent CSB co-fractionating with chromatin. *Error bars* represent S.E. Paired *t* test comparing CSB enrichment in DMSO- *versus* KU-0058948–treated cells ($n = 5$) revealed no significant difference.

PARP1 knockdown significantly reduced the kinetics of CSB–chromatin association following menadione treatment, although ~90% of the CSB eventually associates with chromatin after a 1-h menadione treatment (Fig. 5, *B–D*). To confirm this finding, we repeated the experiments in control and PARP1 knockdown cells, either untreated or treated with menadione for 20 min (average ~96% knockdown, $n = 11$). We found a drop from ~40% CSB co-fractionating with chromatin in cells treated with control shRNA to ~17% in cells treated with PARP1 shRNA (Fig. S2*A*). A difference was observed whether or not we used BRG1 to normalize the protein levels (compare Fig. S2, *A* and *B*). Together, these results indicate that PARP1 enhances the kinetics of menadione-induced CSB–chromatin association.

PARP1 might facilitate menadione-induced CSB–chromatin association through its ability to directly interact with CSB, or alternatively, PARP1 might do so through its enzymatic activity. To determine the contribution of PARP1 enzymatic activity in menadione-induced CSB–chromatin association, we treated cells with the potent PARP inhibitor, KU-0058948 (Fig. 5, *E–H*). Cells treated with KU-0058948 had less poly(ADP-ribosyl)ation activity, as demonstrated by Western blot analysis using an anti-PAR antibody (Fig. 5*E*). However, we did not observe a significant change in the kinetics of CSB–chromatin association induced by menadione treatment, suggesting that PARP1 may influence CSB–chromatin recruitment through direct protein-protein interaction.

We also examined whether CSB played any role in the global recruitment of PARP1 to chromatin (Fig. S4). However, we did not observe any change of PARP1-chromatin association in cells with or without CSB.

### *PARP1 facilitates the recruitment of CSB to specific genomic loci induced by menadione treatment*

ChIP-seq experiments have revealed that menadione treatment also increases the occupancy of CSB at specific genomic loci (20). To determine whether PARP1 participates in recruiting CSB to these loci in response to oxidative stress, we used ChIP-qPCR to examine CSB occupancy at four of these sites (chrX-1, chrX-2, chr17-1, and chr19-2) in cells treated with shRNA targeting PARP1 (Figs. 6*A* and S5). These loci are the four highest CSB occupancy sites induced by menadione. Chr12-7 was used as a control locus, representing a CSB occupancy site that is independent of menadione treatment (20). These loci lie in introns (chr17-1 and chr19-2), a promoter (chrX-2), or an intergenic region (chrX-1). When the PARP1 protein was reduced to ~15% of its normal level, the menadione-induced occupancy of CSB at these loci was significantly reduced (Figs. 6*A* and S5) (20). On the other hand, the occupancy of CSB at the control locus, chr12-7, was not altered by a decrease in PARP1 protein levels (Figs. 6*A* and S5). Together these results indicate that PARP1 plays a key role in facilitating the recruitment of CSB to specific genomic loci in response to oxidative stress, in addition to playing a role in influencing the kinetics of global CSB–chromatin association following oxidative stress.

We next determined whether the locus-specific CSB occupancy relies upon the enzymatic activity of PARP1. As shown in

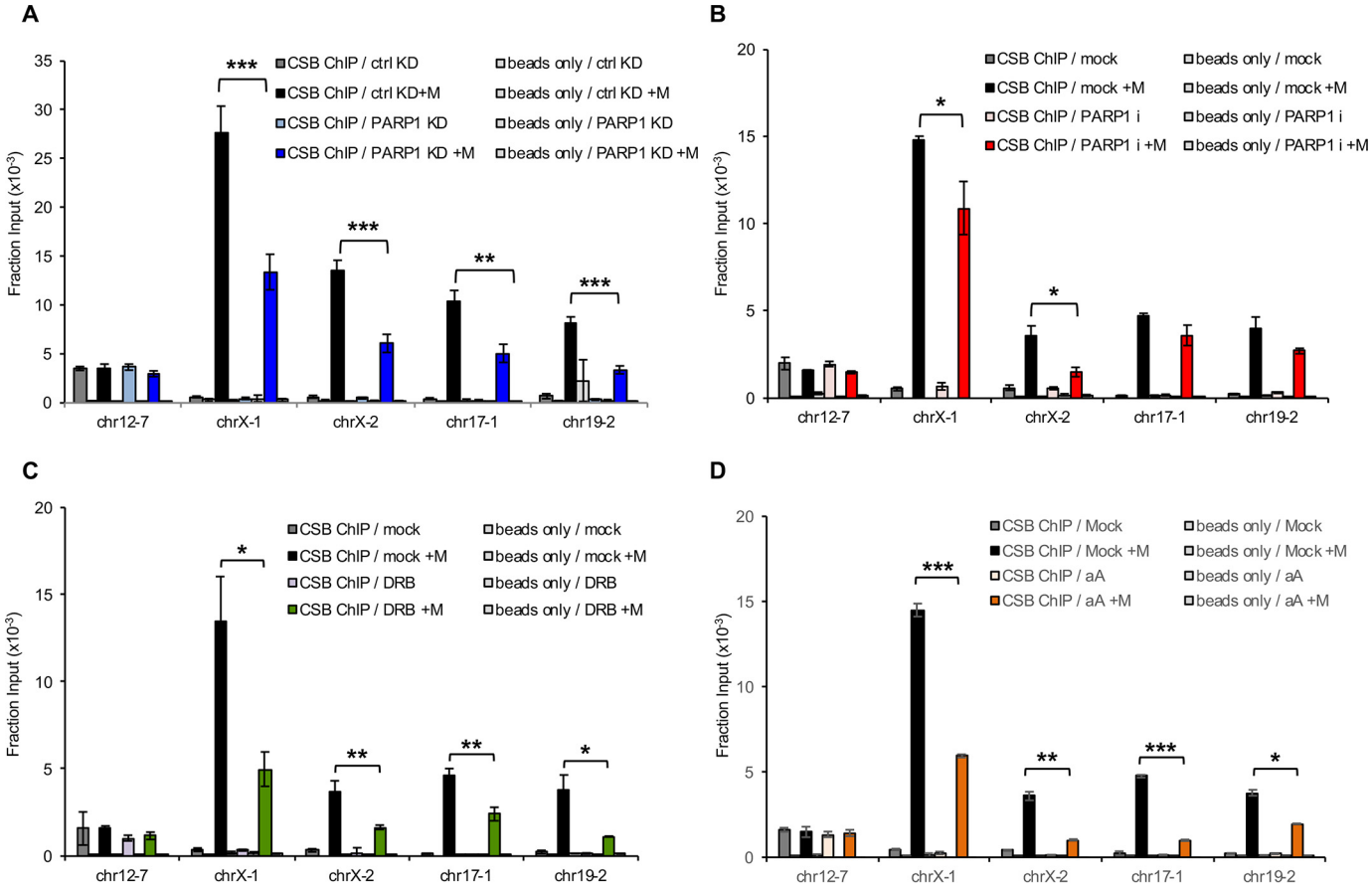


**Figure 6. PARP1 and active transcription contribute to menadione-induced CSB occupancy at specific genomic loci.** Shown are four loci where CSB occupancy is significantly enhanced by oxidative stress (chrX-1, chrX-2, chr17-1, and chr19-2) and a control locus where CSB occupancy is not changed by oxidative stress (chr12-7). *A*, CSB ChIP-qPCR analyses of CS1AN-CSB$^{WT}$ cells expressing a control (*ctrl*) or PARP1 shRNA. Shown are means ± S.E. ($n = 3$). *B*, CSB ChIP-qPCR analyses as above except that cells were exposed to KU-0058948 (*PARP1 i*) or DMSO for 1 h prior to menadione treatment. Shown are means ± S.E. ($n = 2$). *C*, CSB ChIP-qPCR analyses of cells exposed to DRB or DMSO for 1 h prior to menadione treatment. Shown are means ± S.E. ($n = 2$). *D*, ChIP-qPCR analyses of CSB enrichment at specific genomic loci in cells without (*mock*) or with α-amanitin (*aA*) treatment prior to menadione treatment. Cells were treated with 1 mg/ml α-amanitin for 1 h prior to menadione treatment for 20 min. Shown are means ± S.E. ($n = 2$). Paired *t* tests compare CSB enrichment (*, $p \leq 0.05$; **, $p \leq 0.01$; ***, $p \leq 0.001$).

Fig. 6*B*, after treating cells with KU-0058948, we observed a significant decrease in CSB occupancy at chrX-1 and chrX-2, but not chr17-1 and chr19-2. These results indicate that the enzymatic activity of PARP1 contributes to the recruitment of CSB to specific loci but only at a subset of its occupied sites. Interestingly, we found that treating cells with the transcription inhibitor DRB or α-amanitin significantly decreased menadione-induced site-specific CSB occupancy at all four loci, further supporting the notion that CSB functions in transcription regulation at these loci when cells are under oxidative stress (Fig. 6, *C* and *D*).

## Discussion

In this study, we demonstrated that the global chromatin association of CSB induced by oxidative stress does not require ATP-dependent relief of autorepression (Fig. 1) and, therefore, is distinct from the mechanism by which UV irradiation induces CSB–chromatin association for its essential function in TC-NER (37). Our structure-function studies indicate that the N- and C-terminal regions of CSB are required to respond to oxidative stress and that the ATPase domain and C-terminal domain sustain menadione-induced CSB occupancy on a global level (Fig. 2). Importantly, we found that PARP1, a CSB-binding protein, which responds to both single- and double-strand DNA breaks (35, 40), enhances the kinetics of global CSB–chromatin association induced by oxidative stress (Fig. 5). As we observed no apparent increase in the level of γ-H2AX, a marker for DNA double-strand breaks, in cells treated for 30 min with menadione (Fig. 1*A*), these results together support the notion that PARP1 functions in the recruitment of CSB to ssDNA breaks upon oxidative stress (Fig. 7*A*). The majority of single-strand breaks that CSB responds to are unlikely to be the product of BER, as menadione-induced global CSB–chromatin association remains unchanged when the BER proteins OGG1 and APE1 are reduced by ~90 and 70%, respectively (Fig. 4). However, we cannot exclude completely the possibility that the remaining protein participates in CSB recruitment. These observations, therefore, suggest that PARP1 may enhance the recruitment of CSB to sites of ssDNA breaks directly generated by reactive oxygen species through menadione treatment (Fig. 7*A*) (38). Accordingly, we would like to propose that one major function of CSB in cells exposed to oxidative stress is to cooperate with PARP1 in ssDNA break repair.

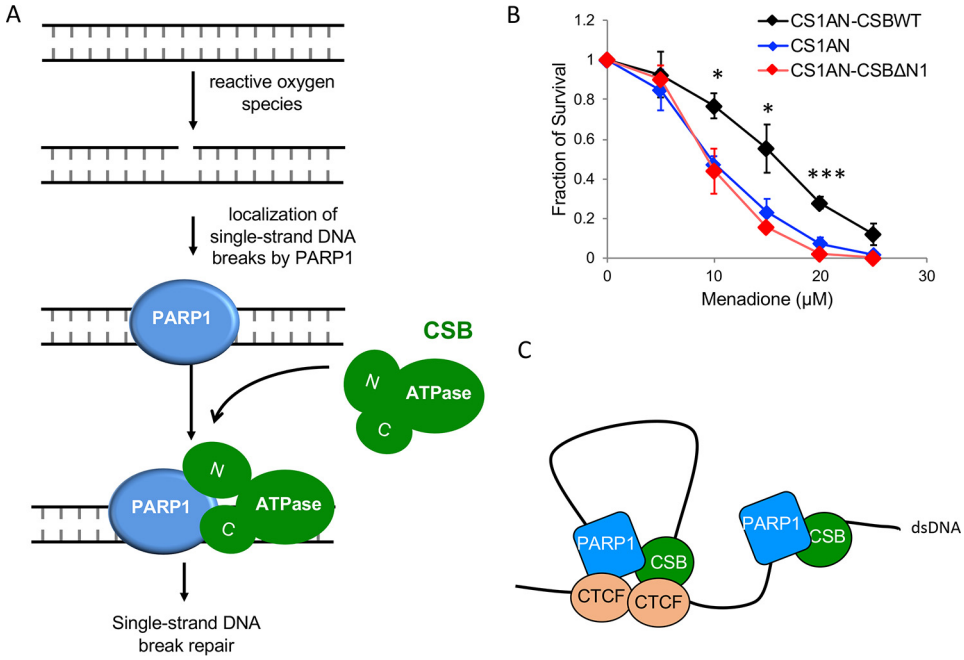


**Figure 7. Models for CSB functions during oxidative stress.** *A*, ssDNA breaks generated by reactive oxygen species are recognized by PARP1. Localization of PARP1 to single-strand breaks facilitates the recruitment of CSB. CSB binds chromatin through its ATPase domain. Upon oxidative stress, PARP1 binds to the CSB N- and C-terminal regions; this interaction exposes a chromatin interaction surface in the C-terminal region of CSB that stabilizes CSB–chromatin association. CSB may function to make the chromatin landscape more permissible for DNA repair and/or to regulate repair-protein retention at sites of repair. *B*, menadione sensitivity assays. The chromatin remodeling–deficient CSBΔN1 derivative does not complement the menadione sensitivity of CS1AN-sv cells. Paired *t* tests compare CS1AN-CSB$^{WT}$ with CS1AN-CSBΔN1 ($n = 5$; *, $p \leq 0.05$; ***, $p \leq 0.001$). *C*, menadione-induced CSB occupancy at specific genomic loci depends on PARP1 (this study) and CTCF (20). These proteins may likely organize higher-order chromatin structure to mount a transcriptional response to oxidative stress.

This model shown in Fig. 7*A* is consistent with the observation of Menoni *et al.* (32), where OGG1 was not required for the recruitment of CSB to locally induced oxidative DNA damage generated by photoactivation of Ro-19-8022. Furthermore, as we found that PARP1's enzymatic activity is not required for the global CSB–chromatin association induced by menadione, a result suggesting that the enhanced chromatin association kinetics mediated by PARP1 is likely the result of direct protein-protein interaction (Fig. 5).

The global CSB–chromatin association induced by menadione treatment differs from UV-induced CSB–chromatin association (37) in that the latter requires ATP hydrolysis by CSB, inducing a conformational change in CSB that exposes a chromatin-interacting domain in the C-terminal region. Our results are consistent with a model in which the association of PARP1 with CSB leads to the exposure of a chromatin-binding domain within the C-terminal region, which occurs in an ATP-independent manner. *In vitro* binding assays by Thorslund *et al.* (35) identified two regions of CSB that interact with PARP1; one lies between residues 2 and 341 and the other lies between residues 953 and 1204. CSB$^{2-341}$ is part of the N-terminal region, and CSB$^{953-1204}$ spans part of the ATPase domain and the C-terminal regions. Given that the ATPase domain and C-terminal regions contain DNA-binding surfaces (37), our results are consistent with a model in which PARP1 brings CSB to chromatin via direct protein-protein interaction, and CSB uses its ATPase domain and C-terminal region to further stabilize its association at sites of ssDNA damage created by menadione treatment. In agreement with this model, CSB-C lacks one of the PARP1-binding regions, which may account for the delayed kinetics of chromatin association. Although sufficient to bind to PARP1 *in vitro* (35), CSB-N lacks chromatin-binding domains and thus fails to associate with chromatin upon menadione treatment (Fig. 2*D*). Moreover, our observation that DRB does not affect menadione-induced global CSB–chromatin association (Fig. 3) suggests that sites of DNA lesions where CSB binds upon oxidative stress are independent of transcription regulation. This is in sharp contrast to the essential function of CSB in TC-NER, where CSB is delivered to bulky DNA lesion-stalled transcription (41). In the case of TC-NER, when cells are treated with DRB, CSB is not recruited to chromatin after UV irradiation (Fig. 3*C*).

The repair of ssDNA breaks occurs rapidly, within minutes (42, 43). A study by Bryant *et al.* (44) reveals that there are two components of ssDNA repair, an initial fast repair phase with a $t_{1/2}$ of 5–6 min followed by a slow repair phase, proposed to be the repair of ssDNA breaks generated by base-excision DNA repair. On average, one PARP1 molecule scans ~10 nucleosomes of chromatin. This rapid scanning function is believed to enable PARP1 to quickly detect DNA damage (45). Therefore, a delay of 10–15 min in CSB recruitment would be significant relative to PARP1 function in ssDNA repair.

Based on the work of Aherne and O'Brien (38), treating Caco-2 cells with 10 $\mu$M menadione for 30 min creates 348 ± 8 ssDNA breaks, as determined by the comet assay. One possible reason that we did not see increased menadione-induced PARP1-chromatin association is that the fraction of PARP1 binding to single-strand breaks generated by menadione is small relative to the total number of PARP1 molecules performing additional functions. It is also important to note that PARP1

binds to chromatin through multiple domains. For example, PARP1 binds to nucleosomes through its affinity to core histones via its C-terminal region, whereas PARP1 binds to DNA lesions through its zinc fingers.

We also found that $CSB^{\Delta 245-365}$ (CSBΔN1), a CSB derivative that is devoid of any chromatin remodeling activity (39), cannot complement the menadione sensitivity of CSB-deficient cells (Fig. 7*B*). This indicates that the chromatin remodeling activity of CSB is required for CSB's function in the repair of menadione-induced DNA damage, the transcriptional response to oxidative stress, or both. In the case of DNA repair, CSB may function to displace PARP1 to facilitate ssDNA break repair, as proposed by Scheibye-Knudsen *et al.* (36). Additionally, our results with CSBΔN1 (Fig. 7*B*) suggest that CSB may facilitate single-strand break repair by opening up chromatin structure. Indeed, prior studies have shown that PARP1 can recruit other chromatin-remodeling complexes, such as ALC1, CHD2 and SNF2h, to facilitate DNA repair (46–49).

Previously, we had shown that menadione treatment promotes the occupancy of CSB at specific loci throughout the genome, with a significant enrichment in promoters and sites containing the binding motifs of the CTCF transcription factor and that this site-specific occupancy likely reflects a role that CSB plays in mounting a transcriptional response to oxidative stress (20). Here, we have shown that decreasing PARP1 protein levels can significantly decrease the menadione-induced enhancement of site-specific CSB occupancy (Figs. 6*A* and S5). PARP1 has been suggested to regulate transcription through multiple mechanisms (50, 51); therefore, decreased PARP1 levels may reduce transcription at specific loci, which may lead to decreased CSB occupancy at these sites (Figs. 6*A* and S5). This hypothesis is supported by our observation that inhibiting RNA pol II transcription elongation with DRB or α-amanitin also decreases the enhancement of site-specific CSB occupancy induced by menadione (Fig. 6, *C* and *D*). Interestingly, the enzymatic activity of PARP1 was required only at a subset of the loci examined (Fig. 6*B*). PARP1 has recently been found to regulate transcription elongation, in part by ADP-ribosylating, thus inhibiting the negative elongation factor (NELF) (45). Our results are consistent with the notion that the requirement for PARP1 activity in transcription is context-dependent (Fig. 6*A*) (46), suggesting that PARP1 likely enhances CSB occupancy on chromatin through both activity-dependent and -independent mechanisms.

We would like to propose that, in addition to DNA repair as assayed by global chromatin association, CSB likely functions together with PARP1 and CTCF to regulate transcription upon oxidative stress (Fig. 7*C*). Both PARP1 and CTCF can facilitate locus-specific CSB–chromatin association in cells treated with menadione (Figs. 6*A* and S5), and these two proteins have been shown to work together to regulate long-range chromatin structure and transcription regulation (52). Therefore, menadione-induced locus-specific CSB–chromatin association may represent sites where CSB functions with PARP1 and CTCF to regulate long-range chromatin interactions to facilitate menadione-induced transcription regulation.

We demonstrated previously that CSB and CTCF can reciprocally regulate each other's occupancy at specific genomic loci upon oxidative stress, and we hypothesized that CSB may cooperate with CTCF by altering 3D genome organization to facilitate the relief of oxidative stress (20). Although the role of this 3D genome reorganization may be to regulate gene expression, this study also opens up the possibility that 3D chromatin reorganization mediated by CTCF and CSB may facilitate the formation of hubs for the repair of ssDNA breaks identified by PARP1.

## Experimental procedures

### Cell culture and treatment protocol

CS1AN-sv cells and CS1AN-sv cells stably expressing CSB or mutant CSB proteins were maintained in DMEM/F12 supplemented with 10% FBS (10, 39). 293T cells were maintained in DMEM supplemented with 10% FBS. All cells were cultured at 37 °C in 5% $CO_2$. CS1AN-sv cells stably expressing CSB, $CSB^{R670W}$, CSBΔN, and CSBΔC were expressed as described previously (37). CS1AN cells stably expressing CSB-N and CSB-C were generated by transfecting cells with CSB-N or CSB-C expression plasmids and selecting with 600 μg/ml G418 (37). Oxidative stress was induced by treating cells with 100 μM menadione (MP Biomedicals, catalog No. 102259). The PARP inhibitor KU-0058948 hydrochloride (Axon Medchem, catalog No. 2001) was used at a final concentration of 1 μM for 1 h (53). RNA pol II transcription elongation was inhibited by treating cells with 50 μM DRB (Sigma-Aldrich, catalog No. D1916) for 1 h prior to treatment with menadione (37). Cells were treated with the transcription inhibitor α-amanitin (Cayman Chemical Co., catalog No. 17898) at 1 mg/ml for 1 h prior to menadione treatment. Menadione was added directly to the DRB-, α-amanitin-, or KU-0058948 – containing medium. For the UV control experiment, cells were treated with 50 μM DRB for 1 h and then irradiated with 100 J/m$^2$ UV (245 nm) using a Stratalinker (37). Cells were allowed to recover for 1 h prior to processing.

### Protein fractionation and Western blotting

Equal numbers of cells were seeded onto 60-mm dishes and allowed to grow overnight to ~80% confluence. The medium was changed on all plates, and cells were left untreated or treated with 100 μM menadione for the indicated times. Cells were lysed, and proteins were fractionated as described previously (20, 37). Briefly, cells were rinsed with PBS, collected in 200 μl of buffer B (150 mM NaCl, 0.5 mM $MgCl_2$, 20 mM HEPES (pH 8.0), 10% glycerol, 0.5% Triton X-100, and 1 mM DTT) on ice, and centrifuged at 15,000 rpm for 20 min at 4 °C. 150 μl of supernatant was added to 50 μl of 4× SDS sample buffer (soluble fraction), and 200 μl of 1× SDS sample buffer was added to the pellet, which was sonicated for 10 s at 25% amplitude with a Branson 101-135-126 Sonifer (the chromatin-enriched fraction was 1.3 times more concentrated than the soluble fraction). Proteins were run on a NuPAGE™ 4–12% BisTris protein gel (Invitrogen NP0323BOX) with the BenchMark™ prestained protein ladder (Invitrogen 10748-010), and gels were labeled with molecular mass markers (kDa). The loading ratio between the soluble and chromatin-enriched fractions was 1:1.25, if unspecified. Western blotting was developed using SuperSignal West Pico or Dura chemiluminescent substrate (ThermoFisher

Scientific 34580 and 34075), and imaged with a Fujifilm ImageQuant LAS-4000 imager or developed using a Kodak M35A processor. To determine the percentage of CSB co-fractionated with chromatin, the images were scanned and quantified using ImageJ. Determination of percent CSB co-fractionated with chromatin was calculated by normalizing CSB signals to BRG1 signals and adjusting for the 1.25-fold more concentrated chromatin-enriched fraction if not specified (20).

### Lentiviral shRNA knockdown

Mission shRNA targeting OGG1 (TRCN0000314740), APE1 (TRCN0000007958), PARP1 (TRCN0000007932) (54, 55), and a nontargeting shRNA (SHC002) were from Sigma-Aldrich. The virus was produced as described previously (20). Briefly, the virus was produced by co-transfecting 293T cells with shRNA and the third-generation lentiviral packaging plasmids pMGLg-RRE, pRSV-REV, and pMD2.G/VSV. The medium was changed 24 h after transfection, and virus-containing medium was collected 24 h later. The target cell confluence at time of infection was ~20%. The medium was changed 24 h after infection, and cells were harvested at 72 h (PARP1 and APE1) or 96 h (OGG1) post-infection.

### ChIP-Western and ChIP-qPCR analyses

Chromatin immunoprecipitation was carried out as described previously (10, 20). Briefly, ~4 million cells were collected after treatment, fixed, and processed for sonication. The fixed chromatin was sonicated on ice for 12 cycles (30 s on/90 s off) with 40% amplitude using a Branson Sonifier 150T. In general, the size range of sonicated chromatin is between 200 bp and 1 kb with a peak of 500 bp (see Fig. S6 for a representative gel showing DNA fragmentation size range). 5 $\mu$l of monoclonal anti-CSB antibody (1B1) (10) and 5 $\mu$l of protein G-agarose beads (Invitrogen 15920010) were used in each ChIP. Real-time PCR was done using a 7900HT fast real-time PCR System (Applied Biosystems) and SensiFAST™ Sybr Hi-Rox mix (Bioline BIO-92020) following the manufacturer's instructions. Primers are listed in Table S1. Real-time PCR data were analyzed using the $\Delta\Delta$Ct method (56). For ChIP-Western blot analysis, ChIP was conducted as described above following treatment with 100 $\mu$M menadione for 30 min. Samples were reverse cross-linked in 1× SDS sample buffer at 95 °C for 30 min and run immediately on a gel (39).

### Antibodies

Antibodies used for Western blot analysis were rabbit polyclonal anti-CSB antibodies to the N terminus (Jasmine) or C terminus (Libra) (both used at 1:2000) (provided by Dr. Weiner, University of Washington) (37), rabbit polyclonal anti-BRG1 (1:2000) (provided by Dr. Kingston, Massachusetts General Hospital) (37), rabbit polyclonal anti-XRCC1 (1:1000) (Cell Signaling Technology 2735), rabbit polyclonal anti-PARP1 (1:1000) (Cell Signaling Technology 9542), rabbit polyclonal anti-$\gamma$-H2A.X (1:1000) (Cell Signaling Technology 2595), rabbit polyclonal anti-CTCF (1:2000) (Millipore 07-729), mouse monoclonal anti-RNA polymerase II (1:500) (Covance H5), rabbit polyclonal anti-acetyl-histone H3 (1:1000) (Millipore 06-599), rabbit polyclonal anti-histone H3 (1:2000) (Cell Signaling Technology 9715), mouse monoclonal anti-GAPDH (1:10,000) (Millipore MAB374), rabbit polyclonal anti-OGG1 (1:10,000) (Abcam ab124741), rabbit polyclonal anti-APE1 (Cell Signaling Technology 4128S), HRP-conjugated goat anti-rabbit IgG (1:10,000) (Pierce 31460), and HRP-conjugated goat anti-mouse (1:10,000) (The Jackson Laboratory 115-035-044). ChIP was performed using the N-terminal anti-CSB antibody 1B1 (10). Poly(ADP-ribose) was analyzed using mouse monoclonal anti-PAR (1:1000) (Tulip BioLabs 1020/N) and peroxidase-conjugated AffiniPure goat anti-mouse IgG, Fc$\gamma$ subclass 3–specific (1:2000) (Jackson Immunoresearch Laboratories 115-035-209).

### Menadione sensitivity assay

Approximately 100,000 cells were seeded onto 35-mm dishes in DMEM/F12 medium supplemented with 10% FBS and allowed to grow for 24 h at 37 °C. Cells were then given fresh medium and left untreated or treated with the indicated concentrations of menadione for 1 h, after which the menadione-containing medium was removed and fresh medium without menadione was added. Cells were cultured for an additional 24 h, at which point cell viability was determined by trypan blue exclusion using a hemocytometer. The percent survival was calculated as the ratio of treated cells to untreated cells (20).

*Author contributions*—E. L. B., R. J. L., and H. Y. F. conceptualization; E. L. B., R. J. L., K. D., and H. Y. F. data curation; E. L. B., R. J. L., K. D., and H. Y. F. formal analysis; E. L. B. and H. Y. F. funding acquisition; E. L. B., R. J. L., and H. Y. F. investigation; E. L. B., R. J. L., and H. Y. F. writing-original draft; E. L. B., R. J. L., K. D., and H. Y. F. writing-review and editing; R. J. L. and H. Y. F. supervision; R. J. L., K. D., and H. Y. F. methodology; H. Y. F. project administration.

*Acknowledgment—We thank Marisa Bartolomei for the anti-PAR antibodies.*

## References

1. Lehmann, A. R. (1982) Three complementation groups in Cockayne syndrome. *Mut. Res.* **106,** 347–356 CrossRefMedline
2. Nance, M. A., and Berry, S. A. (1992) Cockayne syndrome: Review of 140 cases. *Am. J. Med. Genet.* **42,** 68–84 CrossRef Medline
3. Troelstra, C., van Gool, A., de Wit, J., Vermeulen, W., Bootsma, D., and Hoeijmakers, J. H. (1992) ERCC6, a member of a subfamily of putative helicases, is involved in Cockayne's syndrome and preferential repair of active genes. *Cell* **71,** 939–953 CrossRef Medline
4. Eisen, J. A., Sweder, K. S., and Hanawalt, P. C. (1995) Evolution of the SNF2 family of proteins: Subfamilies with distinct sequences and functions. *Nucleic Acids Res.* **23,** 2715–2723 CrossRef Medline
5. Citterio, E., Van Den Boom, V., Schnitzler, G., Kanaar, R., Bonte, E., Kingston, R. E., Hoeijmakers, J. H., and Vermeulen, W. (2000) ATP-dependent chromatin remodeling by the Cockayne syndrome B DNA repair-transcription-coupling factor. *Mol. Cell. Biol.* **20,** 7643–7653 CrossRef Medline
6. van Gool, A. J., Citterio, E., Rademakers, S., van Os, R., Vermeulen, W., Constantinou, A., Egly, J. M., Bootsma, D., and Hoeijmakers, J. H. (1997) The Cockayne syndrome B protein, involved in transcription-coupled DNA repair, resides in an RNA polymerase II-containing complex. *EMBO J.* **16,** 5955–5965 CrossRef Medline
7. Tantin, D., Kansal, A., and Carey, M. (1997) Recruitment of the putative transcription-repair coupling factor CSB/ERCC6 to RNA polymerase II elongation complexes. *Mol. Cell. Biol.* **17,** 6803–6814 CrossRef Medline

8. Selby, C. P., and Sancar, A. (1997) Cockayne syndrome group B protein enhances elongation by RNA polymerase II. *Proc. Natl. Acad. Sci. U.S.A.* **94,** 11205–11209 CrossRefMedline
9. Balajee, A. S., May, A., Dianov, G. L., Friedberg, E. C., and Bohr, V. A. (1997) Reduced RNA polymerase II transcription in intact and permeabilized Cockayne syndrome group B cells. *Proc. Natl. Acad. Sci. U.S.A.* **94,** 4306–4311 CrossRef Medline
10. Lake, R. J., Boetefuer, E. L., Tsai, P. F., Jeong, J., Choi, I., Won, K. J., and Fan, H. Y. (2014) The sequence-specific transcription factor c-Jun targets Cockayne syndrome protein B to regulate transcription and chromatin structure. *PLoS Genet.* **10,** e1004284 CrossRef Medline
11. Newman, J. C., Bailey, A. D., and Weiner, A. M. (2006) Cockayne syndrome group B protein (CSB) plays a general role in chromatin maintenance and remodeling. *Proc. Natl. Acad. Sci. U.S.A.* **103,** 9613–9618 CrossRef Medline
12. Hanawalt, P. C., and Spivak, G. (2008) Transcription-coupled DNA repair: Two decades of progress and surprises. *Nat. Rev. Mol. Cell Biol.* **9,** 958–970 CrossRef Medline
13. Troelstra, C., Odijk, H., de Wit, J., Westerveld, A., Thompson, L. H., Bootsma, D., and Hoeijmakers, J. H. (1990) Molecular cloning of the human DNA excision repair gene ERCC-6. *Mol. Cell. Biol.* **10,** 5806–5813 CrossRef Medline
14. Venema, J., van Hoffen, A., Natarajan, A. T., van Zeeland, A. A., and Mullenders, L. H. (1990) The residual repair capacity of xeroderma pigmentosum complementation group C fibroblasts is highly specific for transcriptionally active DNA. *Nucleic Acids Res.* **18,** 443–448 Medline
15. Mayne, L. V., and Lehmann, A. R. (1982) Failure of RNA synthesis to recover after UV irradiation: An early defect in cells from individuals with Cockayne's syndrome and xeroderma pigmentosum. *Cancer Res.* **42,** 1473–1478 Medline
16. Bohr, V. A., Smith, C. A., Okumoto, D. S., and Hanawalt, P. C. (1985) DNA repair in an active gene: Removal of pyrimidine dimers from the DHFR gene of CHO cells is much more efficient that in the genome overall. *Cell* **40,** 359–369 CrossRef Medline
17. Mellon, I., Spivak, G., and Hanawalt, P. C. (1987) Selective removal of transcription-blocking DNA damage from the transcribed strand of the mammalian DHFR gene. *Cell* **51,** 241–249 CrossRef Medline
18. Khobta, A., and Epe, B. (2013) Repair of oxidatively generated DNA damage in Cockayne syndrome. *Mech. Ageing Dev.* **134,** 253–260 CrossRef Medline
19. Kyng, K. J., May, A., Brosh, R. M., Jr, Cheng, W. H., Chen, C., Becker, K. G., and Bohr, V. A. (2003) The transcriptional response after oxidative stress is defective in Cockayne syndrome group B cells. *Oncogene* **22,** 1135–1149 CrossRef Medline
20. Lake, R. J., Boetefuer, E. L., Won, K. J., and Fan, H. Y. (2016) The CSB chromatin remodeler and CTCF architectural protein cooperate in response to oxidative stress. *Nucleic Acids Res.* **44,** 2125–2135 CrossRef Medline
21. Pascucci, B., Lemma, T., Iorio, E., Giovannini, S., Vaz, B., Iavarone, I., Calcagnile, A., Narciso, L., Degan, P., Podo, F., Roginskya, V., Janjic, B. M., Van Houten, B., Stefanini, M., Dogliotti, E., and D'Errico, M. (2012) An altered redox balance mediates the hypersensitivity of Cockayne syndrome primary fibroblasts to oxidative stress. *Aging Cell* **11,** 520–529 CrossRef Medline
22. Tuo, J., Müftüoglu, M., Chen, C., Jaruga, P., Selzer, R. R., Brosh, R. M., Jr, Rodriguez, H., Dizdaroglu, M., and Bohr, V. A. (2001) The Cockayne syndrome group B gene product is involved in general genome base excision repair of 8-hydroxyguanine in DNA. *J. Biol. Chem.* **276,** 45772–45779 CrossRef Medline
23. Muftuoglu, M., de Souza-Pinto, N. C., Dogan, A., Aamann, M., Stevnsner, T., Rybanska, I., Kirkali, G., Dizdaroglu, M., and Bohr, V. A. (2009) Cockayne syndrome group B protein stimulates repair of formamidopyrimidines by NEIL1 DNA glycosylase. *J. Biol. Chem.* **284,** 9270–9279 CrossRef Medline
24. Dianov, G. L., and Hübscher, U. (2013) Mammalian base excision repair: The forgotten archangel. *Nucleic Acids Res.* **41,** 3483–3490 CrossRef Medline
25. Parsons, J. L., Dianova, I. I., Allinson, S. L., and Dianov, G. L. (2005) Poly(ADP-ribose) polymerase-1 protects excessive DNA strand breaks from deterioration during repair in human cell extracts. *FEBS J.* **272,** 2012–2021 CrossRef Medline
26. Satoh, M. S., and Lindahl, T. (1992) Role of poly(ADP-ribose) formation in DNA repair. *Nature* **356,** 356–358 CrossRef Medline
27. El-Khamisy, S. F., Masutani, M., Suzuki, H., and Caldecott, K. W. (2003) A requirement for PARP-1 for the assembly or stability of XRCC1 nuclear foci at sites of oxidative DNA damage. *Nucleic Acids Res.* **31,** 5526–5533 CrossRef Medline
28. Abbotts, R., and Wilson, D. M., 3rd (2017) Coordination of DNA single strand break repair. *Free Radic Biol. Med.* **107,** 228–244 CrossRef Medline
29. Dianov, G., Bischoff, C., Sunesen, M., and Bohr, V. A. (1999) Repair of 8-oxoguanine in DNA is deficient in Cockayne syndrome group B cells. *Nucleic Acids Res.* **27,** 1365–1368 CrossRef Medline
30. Tuo, J., Jaruga, P., Rodriguez, H., Bohr, V. A., and Dizdaroglu, M. (2003) Primary fibroblasts of Cockayne syndrome patients are defective in cellular repair of 8-hydroxyguanine and 8-hydroxyadenine resulting from oxidative stress. *FASEB J.* **17,** 668–674 CrossRef Medline
31. Tuo, J., Jaruga, P., Rodriguez, H., Dizdaroglu, M., and Bohr, V. A. (2002) The Cockayne syndrome group B gene product is involved in cellular repair of 8-hydroxyadenine in DNA. *J. Biol. Chem.* **277,** 30832–30837 CrossRef Medline
32. Menoni, H., Hoeijmakers, J. H., and Vermeulen, W. (2012) Nucleotide excision repair-initiating proteins bind to oxidative DNA lesions *in vivo*. *J. Cell Biol.* **199,** 1037–1046 CrossRef Medline
33. Tuo, J., Chen, C., Zeng, X., Christiansen, M., and Bohr, V. A. (2002) Functional crosstalk between hOgg1 and the helicase domain of Cockayne syndrome group B protein. *DNA Repair* (*Amst.*) **1,** 913–927 Medline
34. Wong, H. K., Muftuoglu, M., Beck, G., Imam, S. Z., Bohr, V. A., and Wilson, D. M., 3rd. (2007) Cockayne syndrome B protein stimulates apurinic endonuclease 1 activity and protects against agents that introduce base excision repair intermediates. *Nucleic Acids Res.* **35,** 4103–4113 CrossRef Medline
35. Thorslund, T., von Kobbe, C., Harrigan, J. A., Indig, F. E., Christiansen, M., Stevnsner, T., and Bohr, V. A. (2005) Cooperation of the Cockayne syndrome group B protein and poly(ADP-ribose) polymerase 1 in the response to oxidative stress. *Mol. Cell. Biol.* **25,** 7625–7636 CrossRef Medline
36. Scheibye-Knudsen, M., Mitchell, S. J., Fang, E. F., Iyama, T., Ward, T., Wang, J., Dunn, C. A., Singh, N., Veith, S., Hasan-Olive, M. M., Mangerich, A., Wilson, M. A., Mattson, M. P., Bergersen, L. H., Cogger, V. C., *et al.* (2014) A high-fat diet and NAD(+) activate Sirt1 to rescue premature aging in Cockayne syndrome. *Cell Metab.* **20,** 840–855 CrossRef Medline
37. Lake, R. J., Geyko, A., Hemashettar, G., Zhao, Y., and Fan, H. Y. (2010) UV-induced association of the CSB remodeling protein with chromatin requires ATP-dependent relief of N-terminal autorepression. *Mol. Cell* **37,** 235–246 CrossRef Medline
38. Aherne, S. A., and O'Brien, N. M. (2000) Mechanism of protection by the flavonoids, quercetin and rutin, against *tert*-butylhydroperoxide- and menadione-induced DNA single strand breaks in Caco-2 cells. *Free Radic. Biol. Med.* **29,** 507–514 CrossRef Medline
39. Cho, I., Tsai, P. F., Lake, R. J., Basheer, A., and Fan, H. Y. (2013) ATP-dependent chromatin remodeling by Cockayne syndrome protein B and NAP1-like histone chaperones is required for efficient transcription-coupled DNA repair. *PLoS Genet.* **9,** e1003407 CrossRef Medline
40. Ray Chaudhuri, A., and Nussenzweig, A. (2017) The multifaceted roles of PARP1 in DNA repair and chromatin remodelling. *Nat. Rev. Mol. Cell Biol.* **18,** 610–621 CrossRef Medline
41. Boetefuer, E. L., Lake, R. J., and Fan, H. Y. (2018) Mechanistic insights into the regulation of transcription and transcription-coupled DNA repair by Cockayne syndrome protein B. *Nucleic Acids Res.* **46,** 7471–7479 Medline
42. Fisher, A. E., Hochegger, H., Takeda, S., and Caldecott, K. W. (2007) Poly(ADP-ribose) polymerase 1 accelerates single-strand break repair in concert with poly(ADP-ribose) glycohydrolase. *Mol. Cell. Biol.* **27,** 5597–5605 CrossRef Medline

43. Caldecott, K. W. (2008) Single-strand break repair and genetic disease. *Nat. Rev. Genet.* **9,** 619–631 CrossRef Medline
44. Bryant, P. E., Warring, R., and Ahnström, G. (1984) DNA repair kinetics after low doses of X-rays: A comparison of results obtained by the unwinding and nucleoid sedimentation methods. *Mutat. Res.* **131,** 19–26 Medline
45. Lautier, D., Lagueux, J., Thibodeau, J., Ménard, L., and Poirier, G. G. (1993) Molecular and biochemical features of poly(ADP-ribose) metabolism. *Mol. Cell. Biochem.* **122,** 171–193 CrossRef Medline
46. Gottschalk, A. J., Timinszky, G., Kong, S. E., Jin, J., Cai, Y., Swanson, S. K., Washburn, M. P., Florens, L., Ladurner, A. G., Conaway, J. W., and Conaway, R. C. (2009) Poly(ADP-ribosyl)ation directs recruitment and activation of an ATP-dependent chromatin remodeler. *Proc. Natl. Acad. Sci. U.S.A.* **106,** 13770–13774 CrossRef Medline
47. Ahel, D., Horejsí, Z., Wiechens, N., Polo, S. E., Garcia-Wilson, E., Ahel, I., Flynn, H., Skehel, M., West, S. C., Jackson, S. P., Owen-Hughes, T., and Boulton, S. J. (2009) Poly(ADP-ribose)-dependent regulation of DNA repair by the chromatin remodeling enzyme ALC1. *Science* **325,** 1240–1243 CrossRef Medline
48. Smeenk, G., Wiegant, W. W., Marteijn, J. A., Luijsterburg, M. S., Sroczynski, N., Costelloe, T., Romeijn, R. J., Pastink, A., Mailand, N., Vermeulen, W., and van Attikum, H. (2013) Poly(ADP-ribosyl)ation links the chromatin remodeler SMARCA5/SNF2H to RNF168-dependent DNA damage signaling. *J. Cell Sci.* **126,** 889–903 CrossRef Medline
49. Luijsterburg, M. S., de Krijger, I., Wiegant, W. W., Shah, R. G., Smeenk, G., de Groot, A. J. L., Pines, A., Vertegaal, A. C. O., Jacobs, J. J. L., Shah, G. M., and van Attikum, H. (2016) PARP1 links CHD2-mediated chromatin expansion and H3.3 deposition to DNA repair by non-homologous end-joining. *Mol. Cell* **61,** 547–562 CrossRef Medline
50. Kraus, W. L., and Lis, J. T. (2003) PARP goes transcription. *Cell* **113,** 677–683 CrossRef Medline
51. Gibson, B. A., Zhang, Y., Jiang, H., Hussey, K. M., Shrimp, J. H., Lin, H., Schwede, F., Yu, Y., and Kraus, W. L. (2016) Chemical genetic discovery of PARP targets reveals a role for PARP-1 in transcription elongation. *Science* **353,** 45–50 CrossRef Medline
52. Zhao, H., Sifakis, E. G., Sumida, N., Millán-Ariño, L., Scholz, B. A., Svensson, J. P., Chen, X., Ronnegren, A. L., Mallet de Lima, C. D., Varnoosfaderani, F. S., Shi, C., Loseva, O., Yammine, S., Israelsson, M., Rathje, L. S., *et al.* (2015) PARP1- and CTCF-mediated interactions between active and repressed chromatin at the lamina promote oscillating transcription. *Mol. Cell* **59,** 984–997 CrossRef Medline
53. Hanzlikova, H., Gittens, W., Krejcikova, K., Zeng, Z., and Caldecott, K. W. (2017) Overlapping roles for PARP1 and PARP2 in the recruitment of endogenous XRCC1 and PNKP into oxidized chromatin. *Nucleic Acids Res.* **45,** 2546–2557 Medline
54. Wu, P. K., Wang, J. Y., Chen, C. F., Chao, K. Y., Chang, M. C., Chen, W. M., and Hung, S. C. (2017) Early passage mesenchymal stem cells display decreased radiosensitivity and increased DNA repair activity. *Stem Cells Transl. Med.* **6,** 1504–1514 CrossRef Medline
55. Ma, W., Halweg, C. J., Menendez, D., and Resnick, M. A. (2012) Differential effects of poly(ADP-ribose) polymerase inhibition on DNA break repair in human cells are revealed with Epstein-Barr virus. *Proc. Natl. Acad. Sci. U.S.A.* **109,** 6590–6595 CrossRef Medline
56. Schmittgen, T. D., and Livak, K. J. (2008) Analyzing real-time PCR data by the comparative Ct method. *Nat. Protoc.* **3,** 1101–1108 CrossRef Medline

# Poly(ADP-ribose) polymerase 1 (PARP1) promotes oxidative stress–induced association of Cockayne syndrome group B protein with chromatin

Erica L. Boetefuer, Robert J. Lake, Kostiantyn Dreval and Hua-Ying Fan

*J. Biol. Chem. 2018, 293:17863-17874.*
*doi: 10.1074/jbc.RA118.004548 originally published online September 28, 2018*

---